Radio-Frequency electrical design of the WEST Long Pulse and Load-Resilient ICRH launchers

Walid Helou[a], Laurent Colas[a], Julien Hillairet[a], Daniele Milanesio[b], Patrick Mollard[a], Arnaud Argouarch[c], Gilles Berger-By[a], Jean-Michel Bernard[a], Zhaoxi Chen[d], Jean-Marc Delaplanche[a], Pierre Dumortier[e], Frédéric Durodié[e], Annika Ekedahl[a], Nicolas Fedorczak[a], Fabien Ferlay[a], Marc Goniche[a], Jonathan Jacquot[f], Emmanuel Joffrin[a], Xavier Litaudon[a], Gilles Lombard[a], Riccardo Maggiora[b], Roland Magne[a], Jean-Claude Patterlini[a], Marc Prou[a], Robert Volpe[a], Karl Vulliez[g], Konstantin Winkler[f]

[a]*CEA, IRFM, F-13108 St-Paul-Lez-Durance, France*
[b]*Department of Electronics, Politecnico di Torino, Torino, Italy*
[c]*CEA DAM/DIF/DP2I, Bruyère le Chatel, France*
[d]*Institute of Plasma Physics, Chinese Academy of Sciences, Hefei 230031, China*
[e]*Laboratoire de physique des plasmas de l'ERM, Laboratorium voor plasmafysica van de KMS ï (LPP-ERM/KMS) - Ecole royale militaire-Koninklijke militaire school - BE-1000 Brussels-Belgium*
[f]*Max-Planck Institut für Plasmaphysik, Boltzmannstraße 2, 85748 Garching, Germany*
[g]*Laboratoire dôétanchéité, DEN/DTEC/SDTC, Commissariat à lôénergie atomique et aux énergies alternatives, 2 rue James Watt 26700 Pierrelatte, France*

Three new Ion Cyclotron Resonance Heating (ICRH) launchers have been designed for the WEST project (W-Tungsten Environment in Steady-state Tokamak) in order to operate at 3MW/launcher for 30s and 1MW/launcher for 1000s on H-mode plasmas. These new launchers will be to date the first ICRH launchers to offer the unique combination of Continuous-Wave (CW) operation at high power and load tolerance capabilities for coupling on H-mode edge. The Radio-Frequency (RF) design optimization process has been carried out using Full-Wave electromagnetic solvers combined with electric circuit calculations. Cavity modes occurring between the launchers structures and the Vacuum Vessel Ports (VVP) have been evaluated and cleared out.

Keywords: WEST project, ICRH, S/Z parameters, impedance matching.

1. Introduction

The WEST project aims at modifying Tore-Supra (TS) to an X-point divertor Tokamak, equipped with actively cooled tungsten Plasma Facing Units (PFU), with the goal to test divertor components technologies for ITER [1]. In order to generate ITER-relevant high heat fluxes on its PFU, three new ICRH launchers have been designed for WEST, to operate at 3MW/launcher for 30s and 1MW/launcher for 1000s on ELMy H-mode plasmas. They have been optimized for Hydrogen minority heating scheme in a dipole phasing configuration at 55MHz, with a bandwidth covering the 48-60MHz range. In order to withstand load variations caused by ELMs and ensure Voltage Standing Wave Ratios (VSWR) not exceeding 2:1 at the generators, the design of the launchers is based on the load-resilient concept consisting of a toroidal array of Resonant Double Loops (RDL) with low junction impedance conjugate-T (CT) bridges and internal vacuum capacitors [2]. Matching with internal CT has already proven its load-resilience capabilities on both TS [3] and JET [4], in addition to the external CT [5]. TS Prototype 2007 launcher illustrated good agreement between numerical calculations and measurements [3], but suffered from relatively low coupling, incompatibility with operation at 55MHz (due to small and out-of-range capacitance values) and lack of active cooling. Electromagnetic solvers (HFSS, COMSOL [6] combined to SSWICH code [7] and TOPICA [8,9]), together with electric circuit calculations have been used to optimize the RF design. Starting from the layout of the TS Prototype 2007 launcher, the high power capabilities have been enhanced by optimizing the launchers front-face geometry in order to improve the coupling to the plasma while limiting the capacitors currents (I) and voltages (V) to respectively 850A and 54kV peak, and the electric fields (E) to 2MV/m everywhere inside the launchers (WEST ICRH launchers layout is illustrated in [10]). In addition, the nominal frequency has been increased to 55MHz by reducing the radiating elements reactance. Regarding the rear-part, the bridges and the impedance transformers have been optimized for mechanical considerations [10], as well as to enhance the matching, load-resilience and coupling to ELMy H-mode plasmas. CW capabilities have been achieved by cooling all the launchers components and by validating the mechanical requirements in an iterative manner [10]. Cavity modes excitation between the launchers structures and the VVP has been assessed (in a similar fashion as in [11-13]) and cleared out.

2. Key parameters of the RF design and encountered trade-offs

2.1 Coupling resistance (R_c), coupling resistance per meter (R_{cpm}) and straps mean active reactance (X_s)

author's email: walid.helou@cea.fr

The front-face of each WEST ICRH launcher is an array of 4 straps and is equivalent to a 4-port mutlipole (shaded black-box in Fig.1). The latter one is described by its 4x4 Z-matrix (or any other matrix called in the following as a RF-matrix) and can be derived from Full-Wave modelling using for instance TOPICA [8,9] at the desired frequency and plasma configuration. This matrix gives a full description of all RF quantities at the inputs of the array and is of a great importance for advanced RF analysis as the simulation of matching algorithms.

Yet, in order to estimate the values of the required matching capacitances (C_i, i=1 to 4) and the I/V/E, and ensure, in a first-order analysis, that the requirements are met; it is very useful to reduce the antenna circuit (connection of RF-matrixes) to a simple lumped-element model. By doing so, this enables the use of the formulas described in section 2.2. The impedances $Z_s=R_c+jX_s$ in Fig.1 are defined as follows. For a given straps Z-matrix and excitation current-vector Ī, one can extract R_c (in Ω) using equations 1 to 3 (the voltage vector being the product of the Z-matrix and Ī, P_t is the total radiated power by the N=4 straps). X_s is the mean value of the imaginary parts of the active impedances [14]. Note that 4 identical impedances $Z_s=R_c+jX_s$ crossed by the same current I_{eq} will radiate the same amount of power as does the array when it is excited by Ī. R_{cpm} (in Ω/m) is then deduced from the ratio of R_c and a strap's radiating part's length (D_s = 0.27m). It is worth to state that after some algebra one finds that if Ī has all its components equi-amplitude, R_c would be equal to the mean value of the real parts of the active impedances.

$$\square_{\square} = 2\square_{\square}/(\square\,\square_{\square\square}{}^{\square}) \qquad (1)$$

$$\square_{\square\square} = \square\sqrt{(\sum|\square_{\square}|^{\square})/\square} \qquad (2)$$

$$\square_{\square} = \square\square\square\square\square^{\square}\,\bar{\square}\square/2 \qquad (3)$$

One should stress that many definitions of R_c exist [3,15,16], however the one introduced above is particularly convenient for WEST ICRH launchers as it is valid for any current vector and could be properly compared to the measurements (in the new launchers the voltage probes are located at the straps inputs). Finally, it should be emphasized that, as already outlined in [17], the coupling resistance is mainly a factor of merit indicating that when it is increased (for the same amount of power and at matching) the currents flowing in the capacitors will decrease, however in advanced RF calculations RF-matrixes should be used.

2.2 Capacitances values and I/V/E at matching

After extracting the 4 equal lumped-element impedances $Z_s=R_c+jX_s$, the I/V/E at the straps inputs and the capacitors voltages could be found using equations 4 to 7 (assuming a coaxial connection [18] between the straps and the capacitors). Note that these expressions are given at matching and correspond to peak amplitudes. The capacitances needed to match a poloidal pair of straps (one RDL) could be found using equation 8. In these equations R_{int}, R_{ext}, w_0, L_{self} and Z_{0t} are respectively the internal and external radii of the coaxial connection to the series capacitors, the angular frequency, the capacitors self-inductance and the impedance at the bridge.

$$\square_{\square} = \square\sqrt{\square_{\square}/(2\square_{\square})} \qquad (4)$$

$$\square_{\square} = |\square_{\square}|\square_{\square} \cong \square_{\square}\square\sqrt{\square_{\square}/(2\square_{\square})} \qquad (5)$$

$$\square_{\square} = \square_{\square}/(\square_{\square\square\square}\ln(\square_{\square\square\square}/\square_{\square\square\square})) \qquad (6)$$

$$\square_{\square} = (\square_{\square} \pm \square_{\square})\square\sqrt{\square_{\square}/(2\square_{\square})} \qquad (7)$$

$$\square^{\pm} = \square_{\square}^{\square\square}\square\square_{\square} + \square_{\square}\square_{\square\square\square\square} \pm \square_{\square}\,\square^{\square\square} \qquad (8)$$

$$\square_{\square} = \square\sqrt{2\square_{\square}\square_{\square\square} - \square_{\square}^{\square}} \leq \square_{\square\square} \qquad (9)$$

As expected, one notices that increasing R_c and decreasing X_s are respectively required to decrease the currents and increase the values of the matching capacitances (see section 1). Both increasing R_c and the reduction of X_s are needed to decrease the voltages and electric fields. However, it should be emphasized that increasing R_c has been often accompanied by an increase of X_s. Tradeoff has thus been frequently required between the reduction of the currents on the one hand, and the reduction of the voltages and electric fields and the increase of the capacitances on the other hand.

2.3 ELM-resilience

Lower values of R_c are expected in H-mode (between ELMs) than in L-mode plasmas (partially due to steeper edge-density profiles [19,20]), followed by a strong and fast increase during ELMs [21]. Figure 2 illustrates that in order to validate VSWR<2 at very low coupling (for instance at R_{cpm} = 0.75Ω/m indicated by the red vertical solid lines), small values of R_c should be matched (Fig.2.a and b). However, in these cases, in order to keep VSWR<2 over a wide range of R_c, low impedance values are required at the bridge. Since decreasing Z_{0t} augments the electric fields and harden both the arc-detection at the bridge and the matching (the latter difficulty is due to mutual couplings between the straps [22]), Z_{0t}=3Ω has been chosen as a compromise (see Fig.2.b).

3. RF optimizations and assessment

3.1 Front-face of the launchers

Various parametric scans have been carried out in order to find a compromise between the increase of R_c and the reduction of X_s.

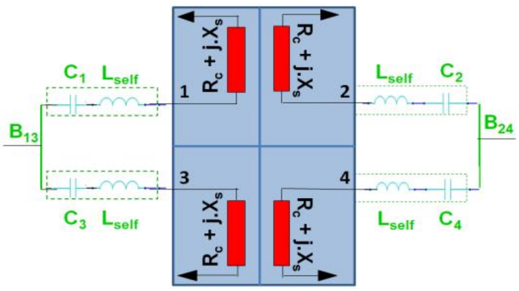

Fig.1. 4-port multipole (shaded black-box), its equivalent lumped-element model (4 impedances $Z_s=R_c+jX_s$), and the matching circuit: the capacitors in series with their self-inductances and ideal bridges (3-branch nodes).

The calculations have been made using HFSS, COMSOL [6] combined to SSWICH code [7] and finally TOPICA [8,9] for geometry milestones. Increasing the straps width decreased both R_c and X_s (in agreement with what has been stated in [23]). This is also the case when increasing the straps thickness. A major modification boosting R_c without altering much X_s has been the reduction of the distance between the straps and the Faraday Screen (FS). Shrinking the TS Prototype 2007's vertical protruding septum also increased R_c, but was accompanied by an increase of X_s (note that an increase of the mutual coupling did not cause major difficulties on the matching). A major modification reducing the value of X_s has been the reduction of the feeder's length. The geometry has been optimized while keeping E<2MV/m even for currents as high as 140% of the maximum allowed current at the strap's input (I_{max}=850A peak).

One should note that the front-face has not been specifically conceived to be optimal in terms of RF-sheaths reduction (as in [24]); however effort has been undertaken to choose the optimal FS [25]. In addition, it should be stressed that, in contrast to the analysis performed in [24], self-consistent RF-sheaths calculations have been carried out for WEST ICRH launchers using SSWICH code. A choice has been made between four FS with different transparencies (FST) and rods tilt angles: tilted rods (7°, FST=0.5), horizontal rods (0°, FST=0.5), tilted-and-dense rods (7°, FST=0.25) and horizontal-and-dense rods (0°, FST=0.25); the third configuration has been chosen as it led to minimal power losses attributed to RF-sheaths over the side limiters. The effect of the FST on R_c and X_s has been found to be negligible for transparencies between 0.25 and 0.5, and its effect on X_s has been validated by low-power measurements on a mock-up.

From figure 3 one clearly sees that starting from the TS Prototype 2007, R_c has been boosted to values even larger than those of the TS Classical launchers [3]. Figure 4 validates the requirements on the matching capacitors at the required frequency band (48-60MHz) and for a scan of coupling resistances. R_c deduced from TOPICA simulations and the corresponding capacitances are also illustrated. TOPICA simulations have been made for various L and H-mode plasma profiles. L-mode profiles (1 to 8, with increasing density) are found from X-mode reflectometry measurements [26] in 2007 on the TS Prototype 2007 launcher, while H-mode profiles are deduced from modelling. In the latter case various Line Averaged Densities (n_e) and distances to the separatrix (D_{sep}) are considered. Note that the capacitors self-inductance of 50nH has been intentionally chosen (datasheets give typically 20-30nH) to insure that the requirements on C are met (mainly that C>40nF).

Concerning the power handling capabilities, using equations 4 to 7 (i.e. at matching), one finds that a launcher would operate at 1MW for R_{cpm}>2.6Ω/m without exceeding the I/V/E limits, but requires high coupling to operate at 3MW (R_{cpm}>7.7Ω/m). It should be noted that for frequencies below 60MHz, the limiting factor is the capacitor's current, while it could be the electric field at higher frequencies.

3.2 Rear-part of the launchers

A major modification has been made on the two-stage (5.3 and 17.7 Ω) Impedance Transformer (IT). Its dimensions have been chosen to transform 3Ω at the bridge's (BR) input to 30Ω at the RF-Window's (RW) input, with the largest bandwidth and minimal current-densities, while respecting both E<2MV/m and the mechanical requirements [10]. Some modifications have been performed to the BR, mainly for mechanical reasons, but it has been verified that they do not alter its electrical response. No modifications have been realized either to the RW or to the service-stub.

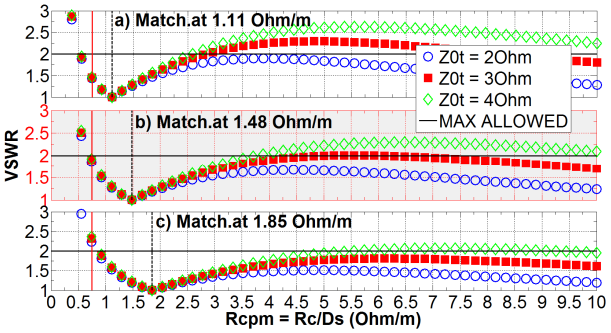

Fig.2. ELM-resilience for various matched coupling resistances (black vertical dashed lines) and impedances at the bridge. The red vertical solid lines correspond to R_{cpm} = 0.75Ω/m.

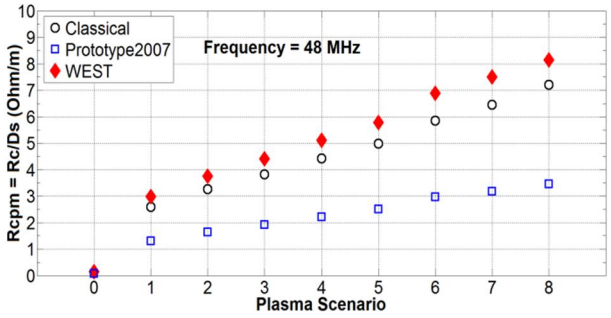

Fig.3. Optimization of R_{cpm} at 48MHz. Plasma Scenario 0 corresponds to simulations in vacuum using HFSS, and those going from 1 to 8 to TOPICA simulations with L-mode plasma profiles with increasing density.

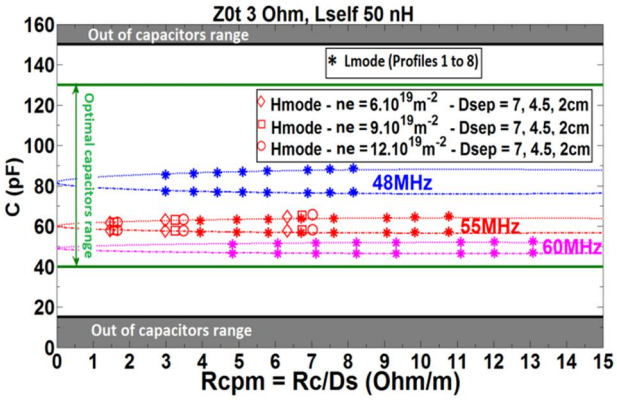

Fig.4. Matching capacitances variation with R_{cpm}. For L-mode, R_{cpm} increases with profiles going from 1 to 8 (increasing density). For H-mode, R_{cpm} increases when n_e increases and D_{sep} decreases. Dashed lines correspond to a scan of R_{cpm}.

Figure 5 illustrates Smith charts with the calculated impedances at the RW's input for various frequencies and BR impedances. It can be noticed that the best-match (VSWR=1) do not correspond to Z_{0t} = 3Ω but rather to 3-j0.5Ω (Fig.5.a); it is believed to be a combined effect of the final IT dimensions differing from the theoretical ones (compatibility with the manufacturing standards) and the RF-Window. Finally, it is known that a slight reactance might have to be added to Z_{0t} (by conveniently setting the capacitors) in order to equalize the straps voltages [4] and enhance the load-resilience [27]; Fig.5 illustrates that this could be achieved without exceeding VSWR=2.

4. Launchers-VVP cavity modes

In [11-13] it has been established for ITER ICRH launcher, theoretically, by simulation as well as experimentally on a reduced-scale mock-up, that cavity modes might be excited between the launcher's plug and the VVP. In the case of WEST ICRH launchers, it has been found using HFSS Eigen-mode solver that a fundamental cavity mode would exist at ~35MHz, followed by a second mode at ~100MHz. Even though those modes are out of the operation range (48-60MHz), it has been found discerning to up-shift the fundamental mode to sup-100MHz frequencies by establishing a conductive path between the launcher's rails and the VVP (Fig.6). Note that in WEST's case, the analyzes were slightly more complicated than in [11-13] since the launcher's structure and the VVP do not form a shorted coaxial line, but rather a cascade of multi-conductor coaxial lines (analytical formulations are less evident).

5. Conclusion

This paper summarizes the RF design of the WEST ICRH launchers conceived by an international team and led by the CEA/IRFM. Starting from the TS Prototype 2007 launcher, the coupling resistance has been boosted and the nominal frequency optimized to 55MHz with a bandwidth covering the 48-60MHz range. Load-resilience has been enhanced by optimizing the bridge and the two-stage impedance transformer. A Faraday Screen with minimal RF-sheaths power losses over the side limiters has been chosen. Note that the generators are being upgraded and the launchers are equipped with several arc-detection systems. Work is ongoing on the simulation of matching and control algorithms using in-house-developed RF network solvers.

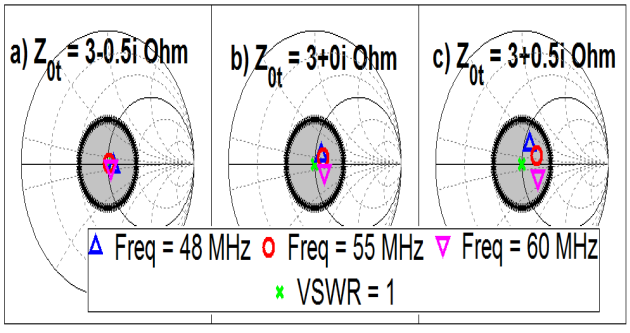

Fig.5. Electrical response of the IT and the RW. The shaded regions correspond to VSWR<2.

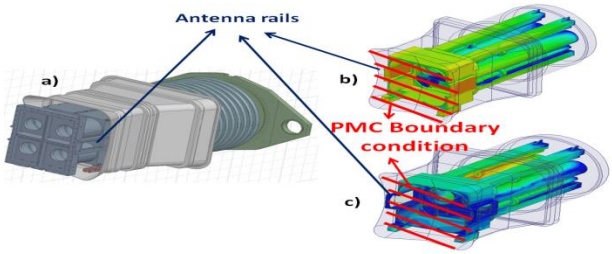

Fig.6. a) The launcher's structure and the VVP. b) Fundamental cavity-mode at ~35MHz without the conductive path. c) Fundamental cavity-mode at sup-100MHz with the conductive path. PMC stands for Perfect Magnetic Conductor.

References

[1] J. Bucalossi et al., Fusion Engineering and Design 89 (2014) 907–912.
[2] G. Bosia, Fusion Science and Technology, Volume 43, Number 2, March 2003, Pages 153-160.
[3] A. Argouarch et al., Fusion Engineering and Design 84 (2009) 275–278.
[4] F. Durodié et al., Plasma Phys. Control. Fusion 54 (2012) 074012 (16pp).
[5] I. Monakhov et al., Nucl. Fusion 53 (2013) 083013 (21pp)
[6] J. Jacquot et al., Plasma Phys. Control. Fusion 55 (2013) 115004 (17pp).
[7] J. Jacquot et al., Physics of Plasmas 21, 061509 (2014).
[8] V. Lancellotti et al., Nucl. Fusion 46 (2006) S476–S499.
[9] D. Milanesio et al., Nucl. Fusion 49 (2009) 115019 (10pp).
[10] K. Vulliez et al., this conference.
[11] F. Louche et al., Nucl. Fusion 49 (2009) 065025 (11pp).
[12] Dumortier et al., Fusion Engineering and Design 88 (2013) 922– 925.
[13] F. Durodié et al., Physics of Plasmas 21, 061512 (2014).
[14] IEEE Standard Definitions of Terms for Antennas, IEEE Std 145-1993(R2004).
[15] M. Goniche et al., Nucl. Fusion 43 (2003) 92–106.
[16] M. Brambilla, Plasma Phys. Control. Fusion 35 (1993) 41-62.
[17] D. Milanesio et al., Plasma Phys. Control. Fusion 49 (2007) 405–419.
[18] N. Marcuvitz, Waveguide Handbook. McGraw-Hill, New York, 1951.
[19] A. Messiaen et al., Plasma Phys. Control. Fusion 53 (2011) 085020 (29pp).
[20] D. Milanesio et al., Plasma Phys. Control. Fusion 55 (2013) 045010 (9pp)
[21] I. Monakhov et al., Proceedings of 15th Top. Conference on RF Power in Plasmas, AIP 694, 2003, pp.146–149.
[22] K. Vulliez et al., Fusion Engineering and Design 74 (2005) 267–271.
[23] F. W. Baity et al., 11th Symposium on Engineering Problems in Fusion Research; 18-22 Nov 1985.
[24] V. Bobkov et al. Nucl. Fusion 53 (2013) 093018 (9pp).
[25] L. Colas et al., Proc. 25th Fusion Energy Conference (FEC 2014), Saint Petersburg, Russia 13-18 October 2014, Poster TH/P6-9.
[26] F. Clairet et al., Review of Scientific Instruments 72, 340 (2001).
[27] P.U. Lamalle et al., Fusion Engineering and Design 74 (2005) 359–365.